

PEDM E/B R&D 11/23/09

Overview.

As discussed above, the edm sensitivity is directly proportional to the electric field strength. We are fortunate that there have been great improvements in sustainable electric fields from R&D for linear colliders, electron guns for ERL, etc., over the last decade. The Pedm experiment is the first large scale DC electric field application to be proposed using the modern techniques. We summarize in Table 1EB our Pedm parameters and what has been achieved for large scale applications previous to the new methods. The electric field strength has low physics and cost risk, i.e., the nominal reliable electric field strength is $\pm 140\text{KV}$ at 2cm separation with the new methods – with R&D we hope to get to $\pm 170\text{KV}$.

Table 1EB. Electrode design parameters for BNL π -K separator, Tevatron pbar-p separator (both designed in the 1980/90s), and Pedm proposal (2009). For the final row, see discussion below.

Parameter	Tevatron pbar-p separator	BNL separator	PEDM
Length	2.6 m	4.5 m	4.8/2.4 m
Gap	5 cm	10 cm	2 cm
Height	0.2 m	0.4 m	0.2 m
Number	24	2	32/64
Max. Cond. HV	$\pm 180\text{ KV}$	$\pm 200\text{ KV}$	$\pm 190\text{ KV}$
Max E 2cm gap	11.4 MV/m	9 MV/m	14 -19 MV/m

Choice of Electrode Material.

The HV breakdown mechanism is dominated by field emission for low gap spacing, and micro-particles [see, for example, H. Fengnian and W. Weihan, IEEE Transactions on Electrical Insulation 25, 557 (1990)] at gap spacing greater than several *mm*. The latter mechanism is that a micro-particle breaks free and accelerates to the other electrode with enough energy to cause melting, which leads to a plasma, and then a spark. Thus the best electrode materials have a high melting point. The macro-particle mechanism predicts a scaling relation with gap of $E_{\text{max}} \propto 1/\sqrt{G}$, $V_{\text{max}} \propto \sqrt{G}$, which works well for gaps of 4-5 *mm* (see Figs. 1-2CM from the above reference). For gaps of 1-2 *mm*, cathode emission is the dominant HV breakdown mechanism, and the maximum electric field becomes independent of the gap, $V_{\text{max}} \propto G$. The breakdown voltage is higher at liquid Nitrogen (LN) temperature than at room temperature in Figs. 1-2CM. In the above micro-particle model, this is because the amount of energy needed to melt the material is larger starting at LN temperature than at room temperature. Stainless Steel (SS) has a higher melting point than Aluminium (1500C vs. 660C), and higher voltages in Figs. 1-2CM. The temperature dependence for cathode emission is given by the Fowler-Nordheim (F-N) approximation:

$$F(T) \approx \frac{\pi kT / d}{\sin(\pi kT / d)} \quad (1\text{CM})$$

where d is the decay width $\approx 0.2\text{eV}$ for metals. Cathode emission is smaller by about 3% at LN temperature compared to room temperature for metals. The Tevatron separator used SS for the cathode and anode. The BNL separator used SS for the anode and anodized Aluminium for the cathode [P. Pile et al., Nucl. Inst. and Meth. A321, 48 (1992)].

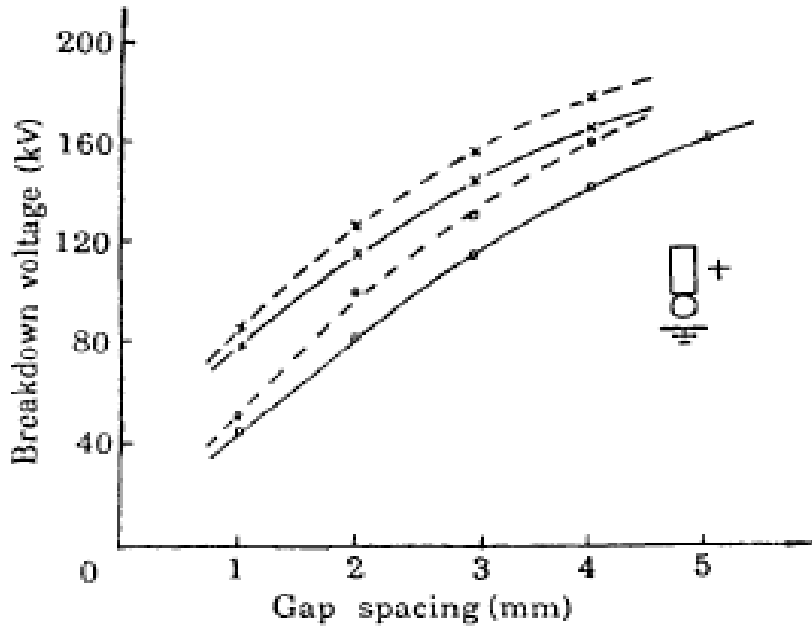


Figure 5.

Positive dc breakdown voltage vs. gap spacing.
 ○ ○ ○ : Aluminum, × × × : stainless steel.
 — : room temperature, - - - : cooled by liquid N₂.

Fig. 1CM. Positive dc breakdown voltage vs. gap spacing for aluminum and stainless steel for room and LN temperatures. The breakdown V starts out linear, and then becomes $V \propto \sqrt{G}$.

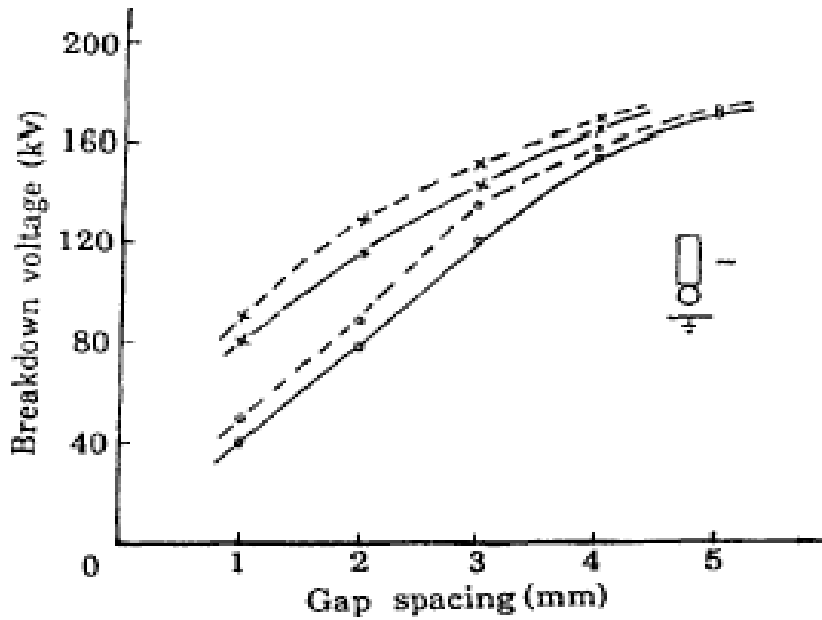


Figure 6.

Negative dc breakdown voltage vs. gap spacing.
 o o o: Aluminum, x x x: stainless steel.
 — : room temperature. - - -: cooled by liquid N₂.

Fig. 2CM. Negative dc breakdown voltage vs. gap spacing for aluminum and stainless steel for room and LN temperatures.

Recently, the CLIC team performed R&D for DC high voltage to gain fundamental understanding of the mechanism of vacuum breakdown [A. Descoeurdes et al., Phys. Rev. STAB 12, 032001 and 092001 (2009)]. They studied small gaps of typically 0.02mm. Their results are very interesting, although not directly relevant to our case of 2cm gap, of course. Since they were trying for basic understanding, they measured a very large number of materials. Fig. 4CM shows the average breakdown electric field. SS gave the highest field. They say: “The ranking cannot be explained by only one dominant material property, but rather by a complex combination of several ones, such as melting point, heat of fusion, thermal conductivity, electrical conductivity, vapor pressure, surface tension, and work function, for example.”

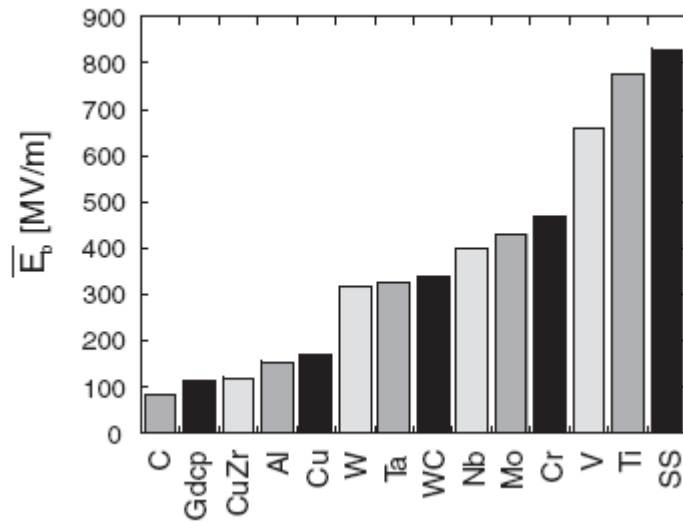


Fig. 4CM. Average breakdown field from A. Descoedres et al., Phys. Rev. STAB 12, 032001 (2009).

Electrode Design.

We anticipate a design very similar to the Tevatron separator SS electrode design shown in Figs. 1-4DS, which have physical parameters close to ours (see Table 1EB).

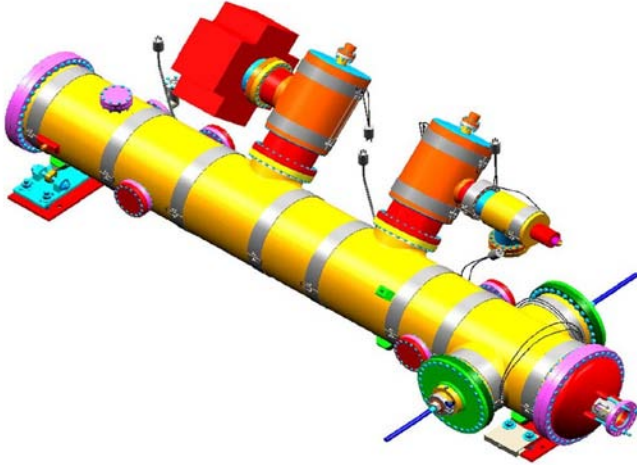


Fig. 1DS. Tevatron separator vacuum tank.

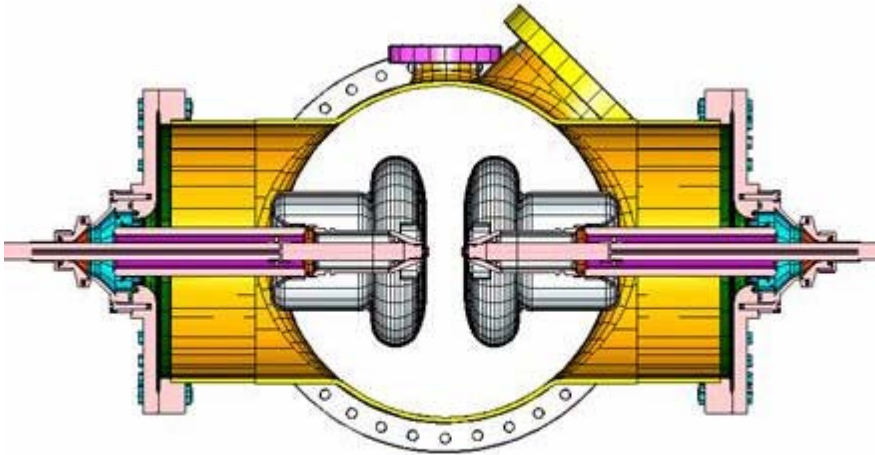


Fig. 2DS. HV feed-through for the Tevatron separator.

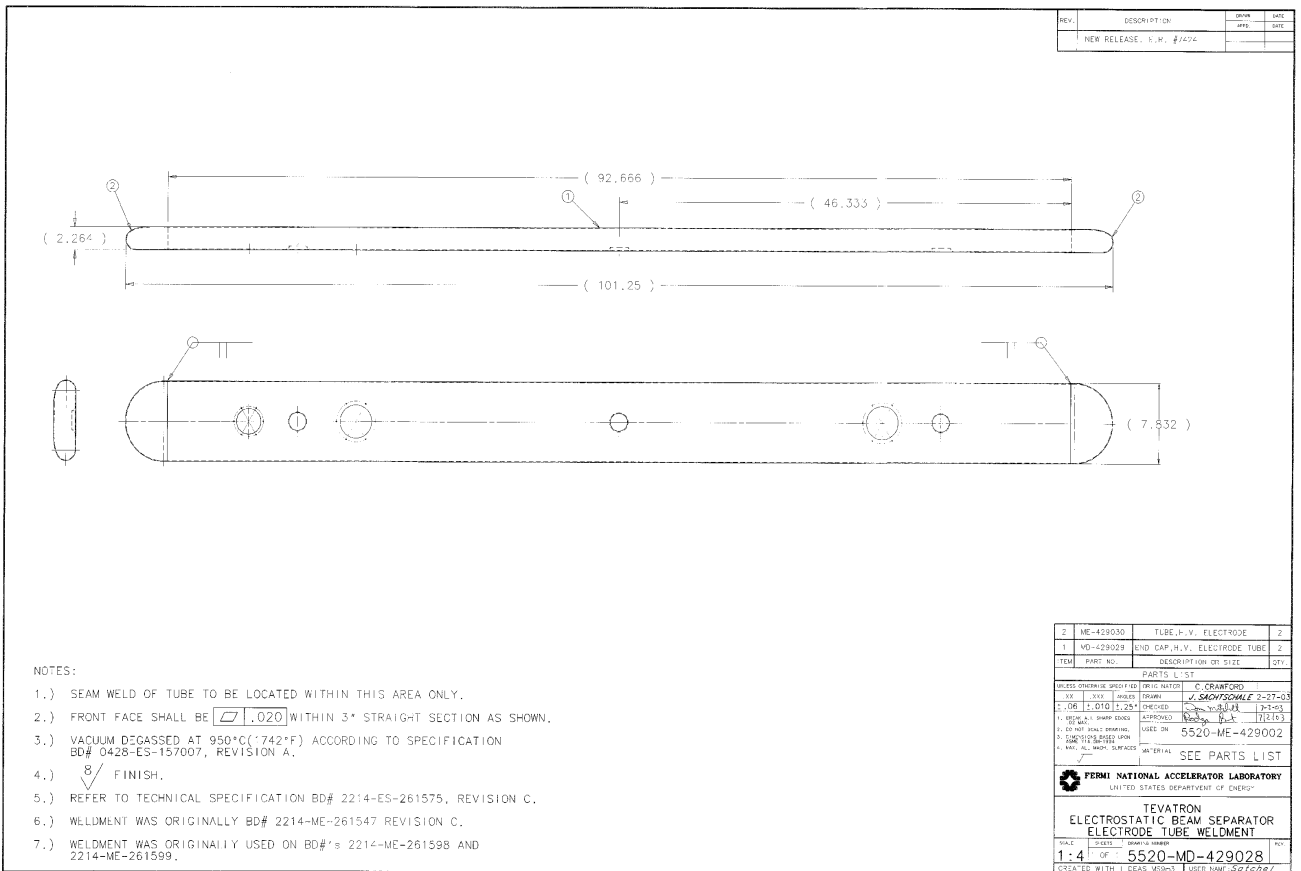


Fig. 3DS. Schematic drawing of the Tevatron separator electrode.



Fig. 4DS. Tevatron separator 101 inch long electrode during construction (back side).

New Methods.

Two new methods for much higher DC HV have been developed: high pressure water rinsing and gas cluster ion implantation. Fig. 1NM shows the improvement for the latter method [D. Swenson et al., Nucl. Inst. Meth. B261, 630 (2007)]. The former method gives similar results. This data is for 5mm gap separation. The next question is: what is the dominant mechanism limiting the maximum electric field with the new methods: field emission, which gives $E_{\max} = C_{fe}$, $V_{\max} = C_{fe}G$, or micro-particles, which gives $E_{\max} = C_{mp}/\sqrt{G}$, $V_{\max} = C_{mp}\sqrt{G}$. We plan to measure E_{\max} as a function of gap in a test setup before and after high pressure water rinsing. Since we know that both field emission and micro-particle mechanisms contribute, we anticipate that it will be somewhere in between (see Fig. 2NM). We will vary the gap from 3mm to 2cm. High pressure water rinsing is the more scalable process up to large area plates than gas cluster ion implantation. There are many facilities which can high pressure water rinse our test plates; however, we will need development of a facility large enough for the final plates for our experiment.

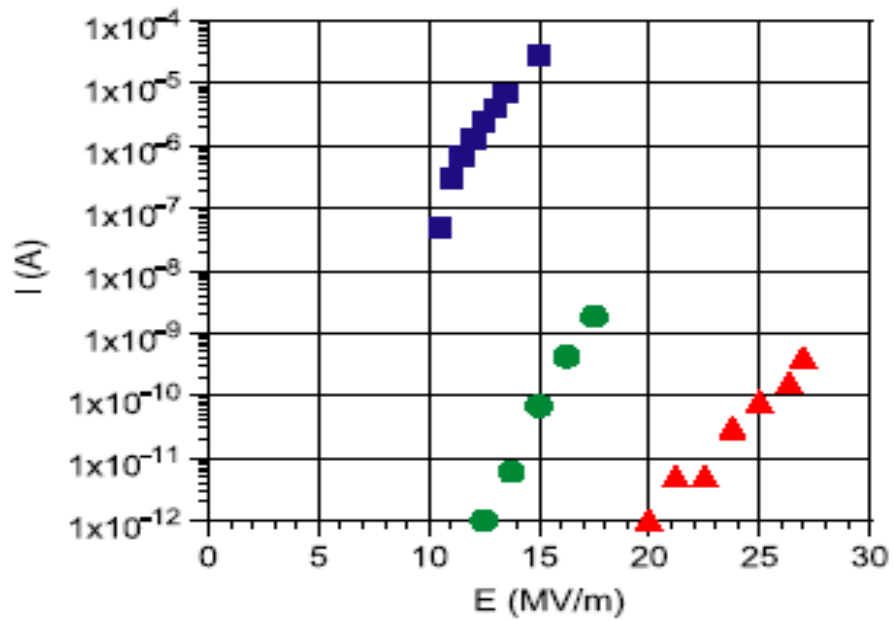


Fig. 4. Field emission current as a function of applied gradient for a 150-mm-diameter stainless steel electrodes: (squares) a typical untreated sample, (circles) first measurement of GCIB treated sample, (triangles) re-measurement of GCIB treated sample after high-voltage conditioning [14].

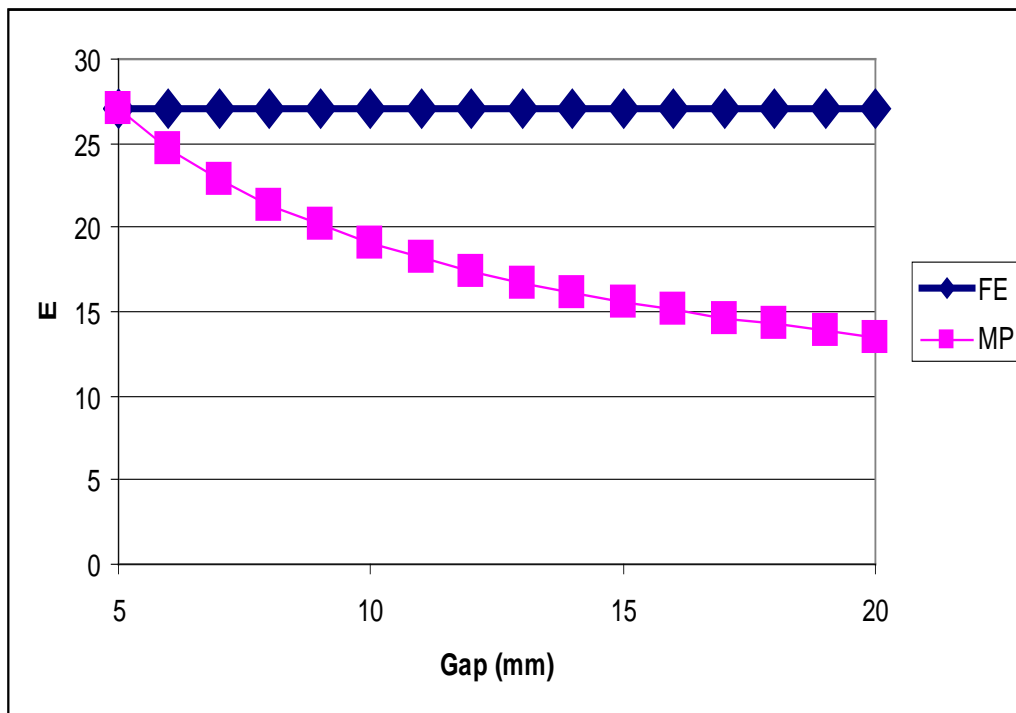


Fig. 2NM. After high pressure water rinsing, we expect that the dependence of E_{\max} on gap will be some combination of the field emission (FE) and the micro-particle (MP) mechanisms.

Sparks.

We discuss here the issue of sparks during the PEDM run. One spark will destroy the SNS neutron edm experiment's squid detectors. They plan for 350KV across a 7cm gap in LHe. The energy of the spark sends a pressure wave through the LHe, which destroys the squid detectors. Their goal is that the probability of a spark is negligible over the lifetime of the experiment.

We spoke with Oleg Prokofiev (Tevatron Beam Separator Group). They have 24 separators, each 2.6m long, 0.2m high with a 5cm gap. They use the separators to separate the proton and anti-proton beams in the Tevatron to get higher luminosity. They didn't use high pressure water rinsing, etc. – it was designed in the last decade. They need a very low spark rate, since a spark loses the Tevatron store, and anti-protons are precious. Before a Tevatron run, they turn on the HV to $\pm 180\text{KV}$, and get finally to about 1 spark per day per separator. They run this way for about a week. During the Tevatron run, they run at $\pm 120\text{KV}$, and get typically one spark every two years per separator. Their design goal was one spark per separator per year. Our design goal is less than one spark every month per unit. Oleg comments: "To reach $\pm 150\text{-}170\text{kV}$ for PEDM E-field plates and have ~ 1 spark/month, conditioning will be performed at voltages 165-190kV. A spark rate at conditioning voltages will be 1 spark/day".

For conditioning, the Tevatron Beam Separator Group starts with current conditioning, then gas conditioning, and finally spark conditioning. An interesting spark conditioning study is described in G.A. Farrall, IEEE Trans. on Elect. Insulation 20(5), 815 (1985). They added capacitors from 10^{-1} to 10^2 nF in parallel to a small area electrode. They found that spark conditioning gave the highest final breakdown voltage for a capacitance of 7nF, but it was a very broad peak: The breakdown voltage for a decade larger or smaller capacitance was similar. The capacitance of one of our module's electrodes is about 0.5nF, at the lower end of their optimal range; however, of course, the optimal capacitance may be quite different for our electrodes. The study for Fig. 3CM used a 27nF capacitor to simulate the stored energy available for a spark for the CLIC cavities.

Wake Fields.

The Tevatron separator wake fields are discussed extensively in J. Crisp and B. Fellenz, FNAL-TM-2202 and K. Ng, Proc. 2003 Part. Acc. Conf. IEEE7803-7739-9. The latter ref. states: "The conclusion points to the fact that the separators actually contribute negligibly when compared with other discontinuities in the Tevatron vacuum chamber, except for the rather large resonance at 22.5MHz. The Tevatron separator 101 inch long plates are $\frac{1}{2}$ wavelength long at 58MHz. The plate and 80 inch power supply cable are $\frac{1}{2}$ wavelength long at 22.5MHz". The Tevatron runs with 0.1A average proton current, while PEDM has only 3mA for IBS reasons. We plan to run at 93MHz RF frequency, so we need to make sure our design is far from resonances. For the Tevatron separator impedance measurements: "Impedance is seen at 22.5 and 67.8 MHz. These frequencies correspond to where the cable and plates are $\frac{1}{2}$ and $\frac{3}{2}$ wavelength long". Their

measured $\text{Re } Z_{L0}/n$ and $\text{Re } Z_{T1}$ impedances were 0.08Ω , 0.01Ω , $0.2\text{M}\Omega/\text{m}$, and $0.04\text{M}\Omega/\text{m}$ at the peak of the 22.5 and 67.8 MHz resonances, respectively. By 100MHz, for example, the impedances are $\approx 2\text{m}\Omega$ and $8\text{K}\Omega/\text{m}$, respectively. These are small compared to other impedances. For example, a strip-line BPM has:

$$\frac{Z_L}{n} \approx 2Z_C \left(\frac{\varphi_0}{2\pi} \right)^2 \frac{l}{R} \quad (1\text{WF})$$

where $\varphi_0/2\pi$ is the fraction of the flux captured by the BPM, l is the length of the strip-line, Z_C is the characteristic impedance, and R is the radius (see for example, R. Shafer, IEEE Trans Nucl. Sci., NS-32 5, 1933, (1985)). As an example, with $Z_C = 50 \Omega$, $\varphi_0/2\pi = 1/\sqrt{2}$, $l = 0.25\text{m}$, and $R = 25\text{m}$, then $Z_L/n = 0.5\Omega$.

From K. Ng's paper *Impedances of Tevatron Separators, Section III: Comparison with BPM*: "Although the Tevatron strip-line BPM is similar in structure to the separator; however, its impedance is completely different. The impedance of one strip-line BPM terminated with the characteristic impedance at the upstream end is:

$$Z_{L0}(\omega) = \frac{1}{2} Z_C \left(\frac{\varphi_0}{2\pi} \right)^2 \left(1 - e^{-j2\omega l/c} \right) \quad (2\text{WF})$$

For a separator plate, there are no terminations on either end. Therefore, the impedance in the above equation does not apply". For example, J. Crisp and B. Fellenz give the illustrative example: "Provided the resonant frequencies of the modes are given by $\omega = n\pi v/l$ and the velocity of the beam is v , then the separator will have no longitudinal impedance". This simple case does not apply, as discussed above, but it illustrates why one can't simply use equ. 2WF to calculate the separator impedance.

Of course, the C-AD beam experts will have to do a complete evaluation for our PEDM ring, but we do not anticipate beam dynamics instabilities, since we have such low beam current. The longitudinal impedance systematic error has been discussed above. The transverse impedance systematic error is discussed next.

Systematic Error due to Image and Wake Fields.

We discuss here the vertical electric and radial magnetic fields seen by the proton bunches due to the electrode image and wake fields. A net vertical electric (radial magnetic) field which is different at the CW vs. CCW bunches is a systematic error for our edm measurement for magnetic (electric) focusing. The bottom line is the net vertical electric and radial magnetic fields will be acceptable as long as the plates are close horizontally and conductors are sufficiently far away vertically for the majority of the ring. If this is obvious, you can skip this section.

Let's consider what happens for a strip-line BPM, since Mike Blaskiewicz pointed out that our E electrodes are, in effect, un-terminated strip-lines. The aqua box in Fig.

1SE represents a resistor with the characteristic impedance Z_c . The voltage across the resistor is:

$$V(t) = \frac{Z_c}{2} \frac{\varphi}{2\pi} \left[I(t) - I\left(t - \frac{L}{\beta c} - \frac{L}{c}\right) \right] \quad (2)$$

(see Robert Shafer, IEEE Tran. Nucl. Sci., Vol. NS-32, No. 5 (1985), for example). The resistor sees the first positive voltage as the beam passes by, and then the second negative voltage at a time $(L/c + L/\beta c)$ later.

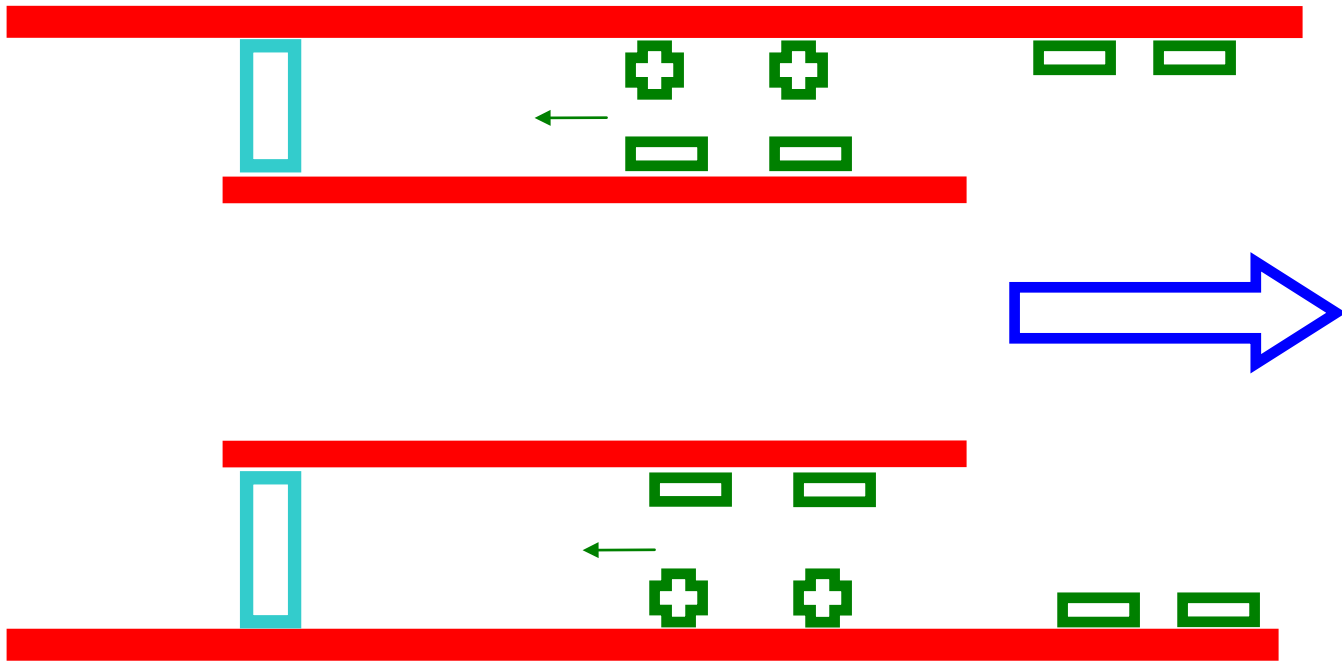


Fig. 1SE. Cartoon of a strip-line BPM resistor (aqua) with resistance equal to the characteristic impedance Z_0 . The bunch has velocity βc , while the backward going electrode/ground charges have velocity c in the absence of dielectric material. This cartoon is for $\beta \approx 1$.

What happens for the case of $\beta \approx 0.6$? We then get the situation shown in Fig. 2SE, shown for a short bunch for clarity. The transverse EM fields between the ground plane and the outside surface of the electrode get to the end of the electrode at $t \approx L/c$ and see an “infinite impedance”, and get “reflected backwards”, using coaxial cable language. When the bunch passes out from the electrode region, it picks up the image charge again in the vacuum chamber. This gives zero electric field in the conductors, as required. The EM fields between the ground plane and the outside surface of the electrode then reflect back and forth until the currents dissipate in a time given by QL/c .

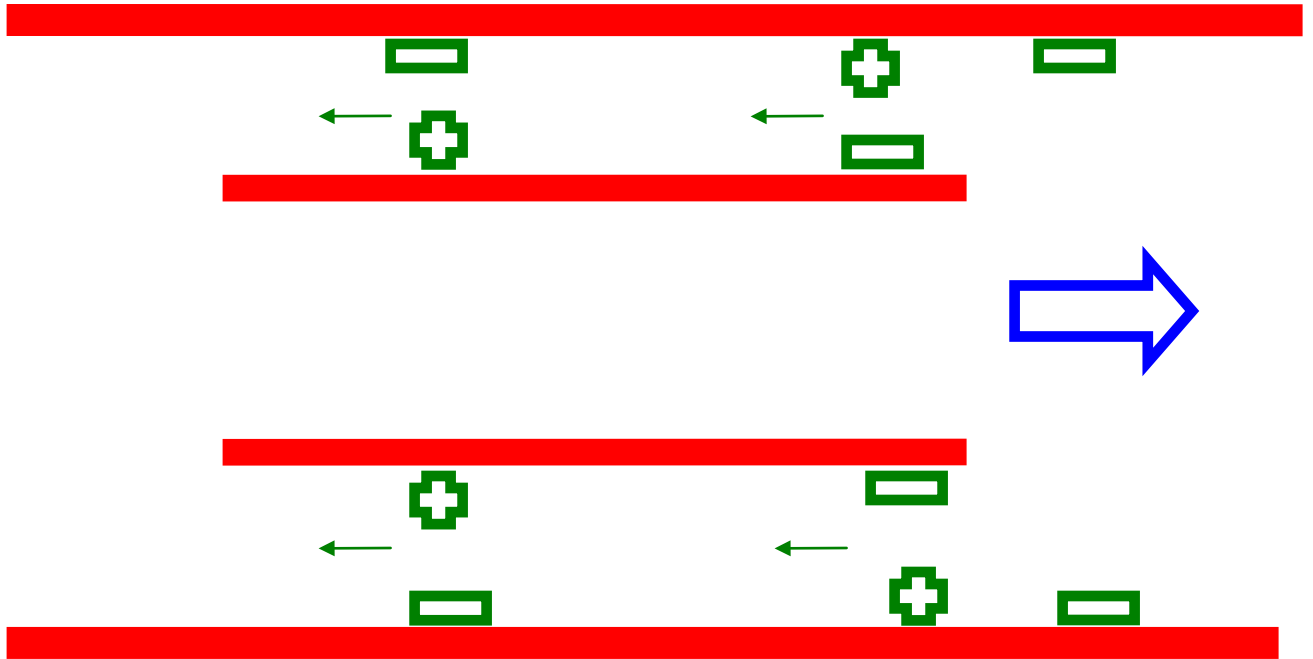


Fig. 2SE. Cartoon electrodes for a short bunch (blue arrow) with $\beta \approx 0.6$. This figure shows a simplified model that does not include power cables, etc.

We are now ready to address the question asked in the first paragraph of this section. The aqua box in Fig. 3SE is a Gauss' Law integration surface. Inside the conductor, $E = 0$. Inside the box, the total charge is zero, if all the negative charge is enclosed. Fig. 4SE shows the negative charge distribution vs. y for an infinite plate. The vertical electric field/radial magnetic field due to the negative charges on the inside of the electrode is acceptable as long as the height of the electrodes is greater than about $10cm$. Obviously, in the fullness of time, this must be calculated correctly with POISSON for the real electrode geometry. There are also charges on the outside of the electrodes, but it's equally positive and negative, and shielded, assuming we avoid the resonances discussed in the last section. So the answer is that there is acceptable net vertical electric field and radial magnetic field due to the image/wake fields from the electrodes, as long as the

beam is at least $\approx 10\text{cm}$ from the top/bottom edges of the electrodes.

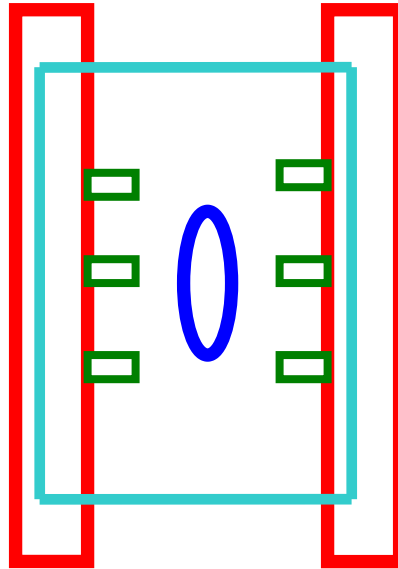


Fig. 3SE. End view of a bunch (blue oval) going through the electrodes showing the image charges on the inside surface of the electrodes. The aqua box is a Gauss' integration surface.

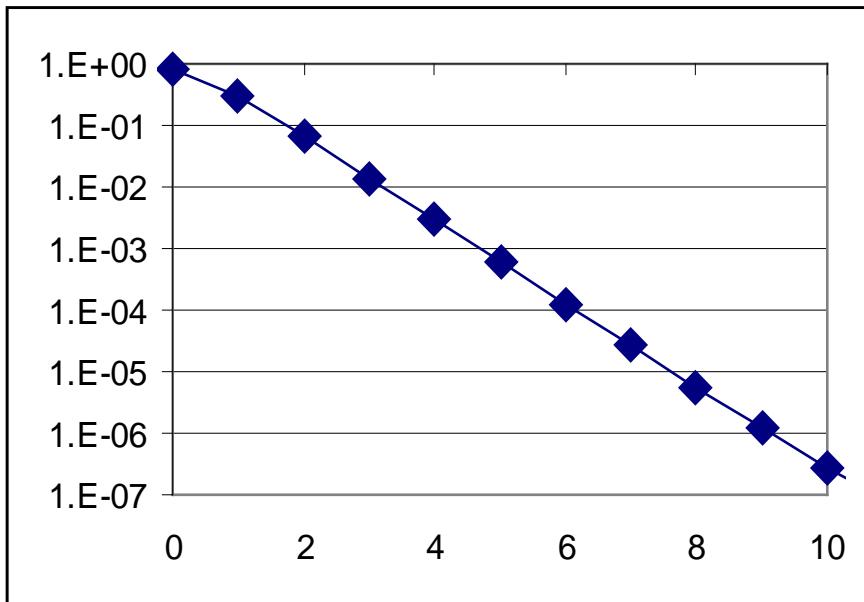


Fig.4SE. Negative charge distribution on the inside of the electrode for an infinitely high electrode vs. y (cm).

Another way to do it is to start with the measured transverse impedances, and then argue that with high enough electrode plates that there is no vertical electric field/radial magnetic field by symmetry considerations.

Patch Effect.

The effective work function varies over the surface of a metal (see Fig. 1PE, as an example). The metallic work function is typically several eV, and the variation is typically several percent. This is negligible compared to the electrode HV of $\approx 170\text{KV}$, and, of course, both the CW and CCW beams see the same effect as they circulate in the CBS ring.

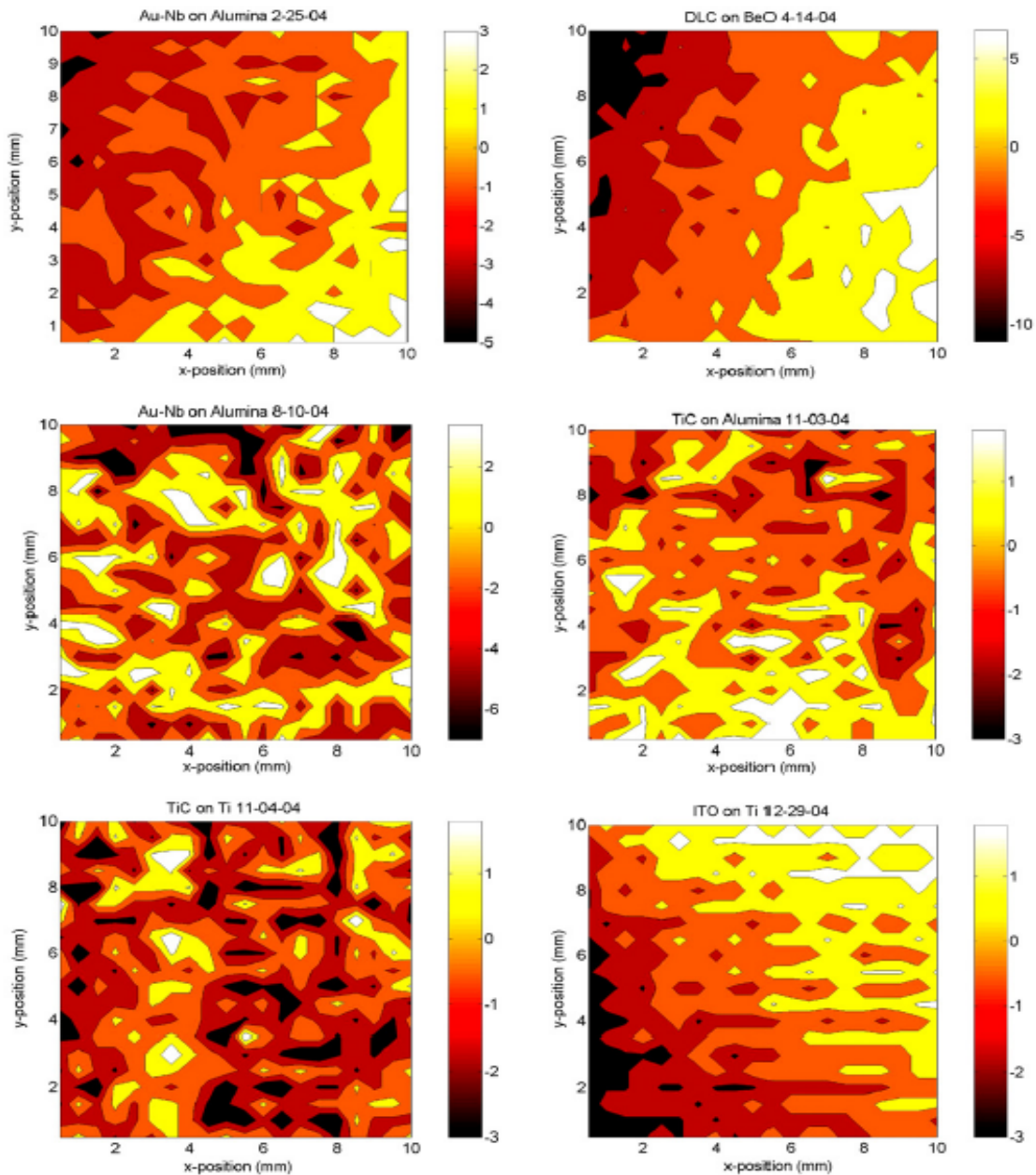


Figure 3. Examples of contour plots of contact potential difference in millivolts over a 10 mm by 10 mm area. The value of offset subtracted/added from each data point is given below. Top left: AuNb on alumina (25-2-04), offset of 15 mV added. Top right: DLC on BeO (14-4-04), offset of 494 mV subtracted. Middle left: AuNb on alumina (10-8-04), offset of 158 mV subtracted. Middle right: TiC on alumina (3-11-04), offset of 328 mV added. Bottom left: TiC on Ti (4-11-04), offset of 331 mV added. Bottom right: ITO on Ti (29-12-04), offset of 275 mV added.

Fig. 1PE. Contact potential difference measurement of various surfaces with the Kelvin probe tip from N. Robertson et al., *Class. Quantum Grav.* 23, 2665 (2006). The stripes seen in the lower right plot were later found to be instrumental.

Focusing

A design by W. Meng of the C-AD Dept. for the quadrupole magnet needed for focusing is shown in Fig. 1FO. The integral Bdl is 1T. The vacuum chamber has outer dimensions of $\approx 195\text{mm}(V)\times 40\text{mm}(H)$. Wuzheng says this design has low technical risk. He is presently working on a design for the sextupole magnet. S. Haciomeroglus, a grad student from Istanbul Technical University, is working on the electric focusing design.

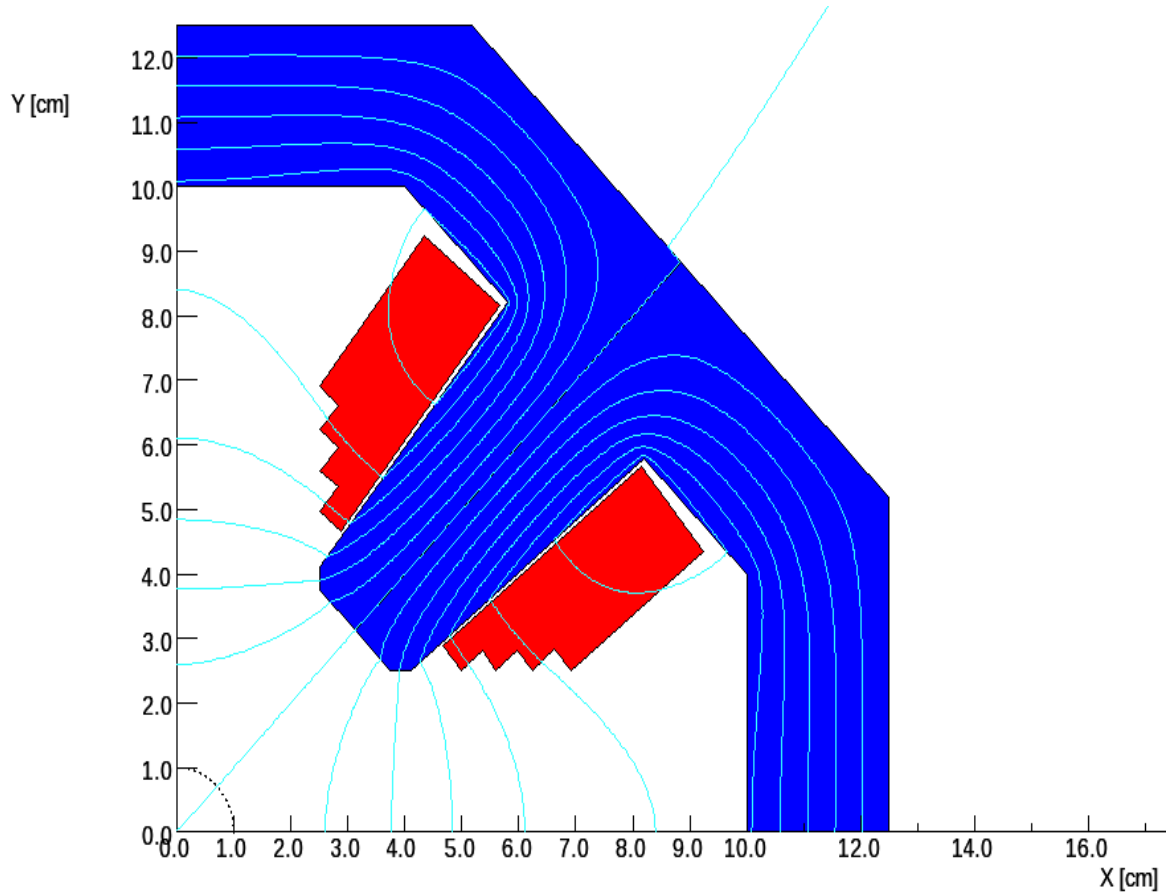


Fig. 1FO. Design of the quadrupole magnet by W. Meng.

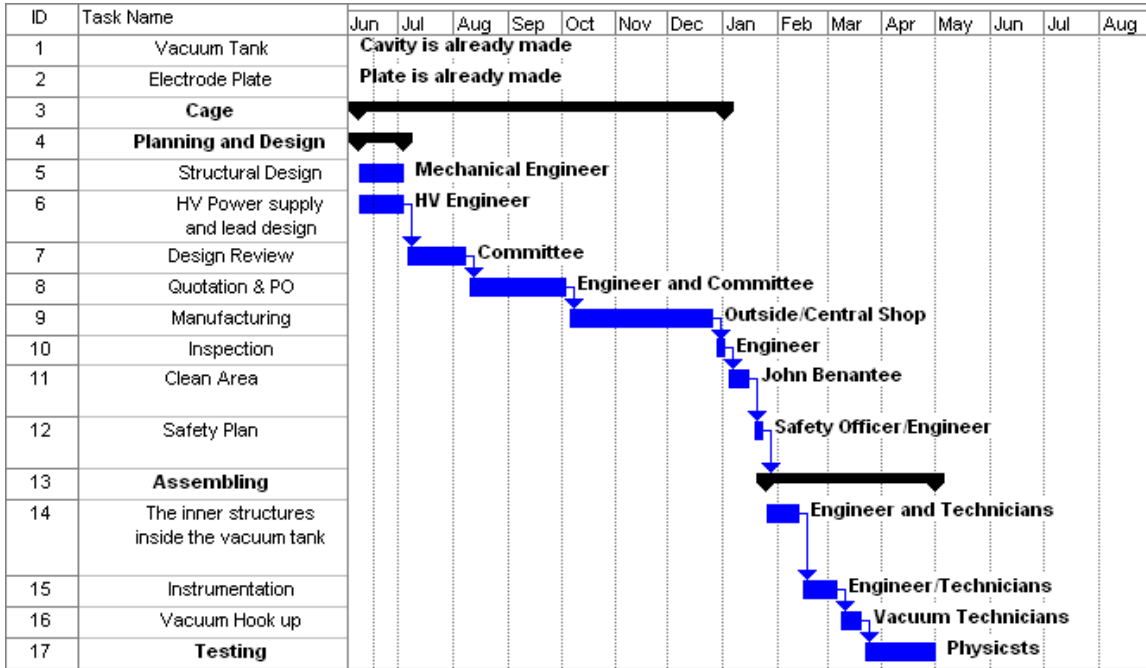
R&D

The E/B R&D consists of:

1. Filling in Fig. 2NM for small area plates,
2. HV testing one electrode module,
3. B R&D consists of Wuzheng Meng's time for the sextupole magnet conceptual design ($\leq 0.3\text{m}$ long, $\approx 20\text{G}/\text{cm}^2$ over $\pm 1\text{cm}$ with uniformity 10^{-3}).

1. Of course, there have been many tests using the new HV methods as discussed above of small area ($\leq 15\text{cm}$ diameter) electrodes at small gaps ($\leq 5\text{mm}$). We need to extend these tests up to 2cm gap. This is expected to take six months of effort of a grad student or post-doc with a technician after the initial testing. The Gantt Chart from last June is shown below. We are basically on schedule. The cost to complete is $0.2\text{M}\$$.

Table1RD.Gantt chart for 1.



2. We would build the first *E* module based on what we learn from 1. The engineering design would start out with the Tevatron separator engineering design and iterate from there. The cost and schedule given in Tables 2-3RD were done by Sumanta Nayak, a C-AD engineer. Oleg Prokofiev, the Tevatron separator team leader, said “one pair of the Tevatron SS electrodes cost \$15K in FY00\$, and the module construction and tests would require a couple hundred thousand FY09\$”. This is a good sanity check of Sumanta’s estimate!

Table 2RD. Cost estimate for 2, not including physicist’s effort.

Name	Dimension (mm)	Design/Plan Hrs	M/L	Man /Ass Hrs	Cost (\$)	Cont (%)	Final Cost
Electrode Plate	2400 X 200 x 20	35	SS304	70	22037	25	27546
Vacuum Tank	460 dia X 2400 Lth X 20 Thk	80	SS304	200	28594	25	35742
Vacuum Tank End Flange	460 dia X 20 thk plate	15	SS304	30	10810	25	13513
Ports	Assume 8" (200) size	10	SS304	18	28362	25	35453
The Vacuum Tank assemble				50	5000	25	6250
Frame assembling & with Plate				30	3000	25	3750

Inner Structure Support System		75	100	27500	75	48125
Gauges				15000	50	22500
Vacuum Equipment	500 l/s Ion Pumps with controller			18000	10	19800
	Turbo Pump			20000	15	23000
	Bake out card			20000	15	23000
	Blankets			35000	15	40250
Vac Equip hook up			40	4000	25	5000
Instrumentation and Testing			100	35000	50	52500
Total				272303		357699

Table3RD. Gantt chart for 2. The start date is arbitrarily set at Jan.1.

